

Telemanipulation of Snake-Like Robots for Minimally Invasive Surgery of the Upper Airway

Ankur Kapoor¹, Kai Xu², Wei Wei², Nabil Simaan², and Russell H. Taylor¹

¹ Johns Hopkins University

kapoor, rht@cs.jhu.edu

² Columbia University

kx2102, ww2161, ns2236@columbia.edu

Abstract. This research focuses on developing and testing the high-level control of a novel eight DOF hybrid robot using a DaVinci master manipulator. The teleoperation control is formulated as weighted, multi objective constrained least square (LS) optimization problems - one for the master controller and the other for the slave controller. This allows us to incorporate various virtual fixtures in our control algorithm as constraints of the LS problem based on the robot environment. Experimental validation to ensure position tracking and sufficient dexterity to perform suturing in confined spaces such as throat are presented.

Minimally invasive surgery (MIS) of the chest and abdomen provide multiple ports to access the anatomy and allows large motions at the proximal joints of telesurgical slave robots. Compared to MIS of the chest and abdomen, it is vital to minimize the motions of the proximal joints in single entry port MIS due to strict space limitations. In addition, the slave robots must have a high distal dexterity and a large number of DOF. This paper presents a general high-level control method for telemanipulation using a linear least square optimization framework. This framework allows easy incorporation of virtual fixtures in high-DOF telesurgical systems for single entry port MIS. The validation of our framework is performed on a novel system for MIS of the throat [1] using a DaVinci master manipulator in our laboratory.

MIS of the throat is characterized by a single entry port (patient's mouth) through which surgical tools operate. Current manual tools are hard to manipulate precisely, and lack sufficient dexterity to permit common surgical tasks such as suturing. This clinical problem motivated the development of a novel system for MIS of the upper airway. Our proposed solution is a telesurgical robot with a hybrid slave manipulator that has a snake-like unit (SLU) at its distal end, which provides high tool-tip dexterity. In previous works [2–5] novel telesurgical slave robots implementing snake-like units for distal dexterity enhancement were presented, but few address the issue of human interfaces to these complex mechanisms. Csencsits et al. [6] evaluated interfaces for snake-like devices using joysticks. Our method allows the addition of virtual fixtures to enable intuitive control of snake-like devices by a human user. Moreover, virtual fixtures can be used to augment MIS tasks that require better-than-human levels of precision.

Virtual fixtures (VF), which have been discussed previously in the literature for cooperative robots [7, 8], are algorithms which provide anisotropic behav-

ior to surgeons motion command besides filtering out tremor to provide safety and precision. Virtual fixtures have been implemented on impedance-type teleoperators under various forms in [9–11]. It has been shown that implementing forbidden-region virtual fixtures using impedance control techniques can lead to instability [12]. Moreover, these works are based either on a specific robot type (admittance or impedance) or on a specific task. We present a method that covers implementation of both guidance and forbidden regions and is suitable for both types of robots. In doing this we extend the work of Funda et al. [13] and Li and Taylor [14, 15] to teleoperated systems with impedance-type master robots. This will enable us to implement stable virtual fixtures on these types of robots.

1 Methods

1.1 Control Algorithm Overview

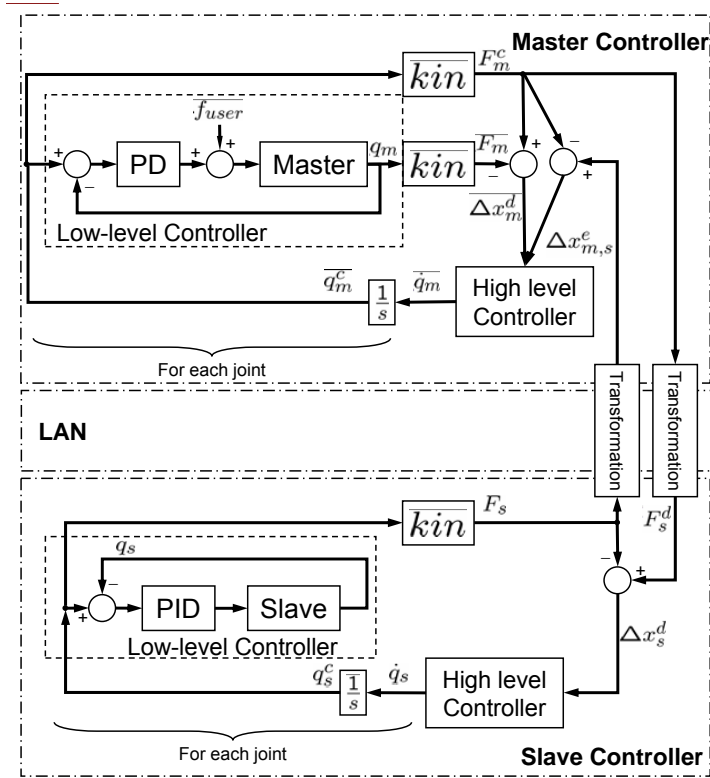


Fig. 1. Block diagram of current implementation of master-slave controller

In this section we outline a new method to address telemanipulation of an admittance-type snake-like robot using an impedance-type robot. To achieve this

we mimic an admittance-type behavior on the master manipulator. The overall structure of the control algorithm is shown in Figure 1. There are separate controllers for the master and the slave connected through a communication network. In the following sections subscripts m and s are used for master and slave respectively and the double subscript m, s is used for variables that are related to both master and slave. The overall method works as follows

1. Individual joints of the manipulator are servoed with low-level controllers (PD or PID) to position set points.
2. A desired Cartesian velocity is calculated for each manipulator. Sections 1.2 and 1.3 discuss the methods to compute the desired Cartesian velocities for master and slave respectively.
3. A constrained least square problem is solved for the joint velocities by the high-level controller. The least square problem has an objective function describing desired outcome. It may also include constraints that consider any motion constraints due to VF, joint limits, and velocity limits. This problem has the general form of

$$\begin{aligned} & \arg \min_{\Delta \mathbf{q}_r / \Delta t} \|(A_r(\mathbf{q}_r, \dot{\mathbf{q}}_r) \cdot \Delta \mathbf{x}_r / \Delta t - \Delta \mathbf{x}_r^d / \Delta t)\|, \\ \text{s.t. } & H_r(\mathbf{q}_r, \dot{\mathbf{q}}_r) \cdot \Delta \mathbf{x}_r / \Delta t \geq \mathbf{h}_r, \quad \text{and} \quad \Delta \mathbf{x}_r / \Delta t = J_r \Delta \mathbf{q}_r / \Delta t \end{aligned} \quad (1)$$

where $r \in \{m, s\}$ for master or slave. $\Delta \mathbf{q}_r$ is the desired incremental motion of the joint variables. The desired incremental motion in Cartesian space, $\Delta \mathbf{x}_r^d = g(\mathbf{f}_{user}, \mathbf{q}_r)$ is a function of user's input, \mathbf{f}_{user} , and joint variables, \mathbf{q}_r . Matrix J_r is the Jacobian of the manipulator. Δt is the small time interval of high-level control loop. Matrices H_r and A_r along with vector \mathbf{h}_r define the behavior of the robot to a given input. Without any constraints, the above constrained LS problem, which is implemented in the high level block shown in Figure 1, is equivalent to resolved rate control.

4. Numerically integrate the joint velocities to arrive at a new set of joint positions. We assume that for each iteration loop, the incremental motions are sufficiently small and $\Delta \mathbf{x}_r / \Delta t = J_r \Delta \mathbf{q}_r / \Delta t$ represents a good approximation to the relationship between $\Delta \mathbf{x}_r / \Delta t$ and $\Delta \mathbf{q}_r / \Delta t$.

1.2 Implementation on Master Manipulator

In this section, we discuss the desired behavior of the master manipulator to an user input and formulate a specific constrained least square problem based on the general form presented in (1). We model the manipulator as a kinematic device having a position $\mathbf{p}_m \in \mathbb{R}^3$ and orientation given by a rotation matrix $R_m \in \mathbb{R}^{3 \times 3}$. The frame $F_m = (R_m, \mathbf{p}_m)$ is computed using the actual encoder joint positions \mathbf{q}_m and the forward kinematics. The frame $F_m^c = (R_m^c, \mathbf{p}_m^c)$ is commanded frame, specified by commanded joint positions \mathbf{q}_m^c (reference set points for servo controller) and the forward kinematics.

Desired Cartesian Velocity In the admittance-type devices a force sensor measures the user input, \mathbf{f}_{user} . The desired Cartesian velocity is computed by

multiplying the user input by the user supplied admittance gain matrix K_a . It has been shown in [16] that for 3 DOF impedance-type robots, under quasi-static condition, the applied user force, \mathbf{f}_{user} can be measured approximately by the position error. We extend it to the 6 DOF case by defining the position and orientation errors as $\mathbf{p}_m^e = \mathbf{p}_m^c - \mathbf{p}_m$ and $R_m^e = R_m^c \cdot R_m^{-1}$, respectively. Further we make use of the small angle approximation to Rodriguez formula for the orientation error,

$$R_m^e = I + (\sin \theta_m) \hat{\omega}_m + (1 - \cos \theta_m) (\hat{\omega}_m)^2 \approx I + \theta_m \hat{\omega}_m; \|\omega_m\|_2 = 1 \quad (2)$$

where $\hat{\omega}_m$ is a skew symmetric matrix corresponding to vector ω_m . Scalar θ_m is the rotation angle about unit vector ω_m . We can replace the force sensor measurement in the admittance control law by a wrench that is a six vector obtained by concatenating \mathbf{p}_m^e and $\theta_m \omega_m$, that is, $\Delta \mathbf{x}_m^d / \Delta t = K_a [\mathbf{p}_m^e; \theta_m \omega_m]$. A small dead-band is used on this error to avoid motion that might arise due to small errors in the servo control.

Objective function In [13] Funda et al presented a constrained least square framework for robot position control. In this work we extend it for teleoperation control of a master-slave. We identify three objective criteria for the tip frame, that are required to achieve desired motion of the tip. First, we require that an incremental motion of master be as close as possible to the desired Cartesian velocity, $\Delta \mathbf{x}_m^d / \Delta t$, which is the function of user input. We express this as: $\min_{\Delta \mathbf{q}_m / \Delta t} \|\Delta \mathbf{x}_m / \Delta t - \Delta \mathbf{x}_m^d / \Delta t\|$.

The second objective criterion concerns the teleoperator that connects the master and slave tips. The slave follows the master positions, but the master must also provide resistance to the user based on the position of the slave and/or the force at the slave tip. For example if the slave is lagging behind, the master can haptically display this to the user by opposing the user's motion that increases the master-slave tracking error. We model this virtual coupling as a spring, which results in: $\min_{\Delta \mathbf{q}_m / \Delta t} \|\Delta \mathbf{x}_m / \Delta t - \Delta \mathbf{x}_{m,s}^e / \Delta t\|$, where $\Delta \mathbf{x}_{m,s}^e$ is a function of both the master and slave positions. We defer the discussion on computation of $\Delta \mathbf{x}_{m,s}^e$ until section 1.3.

Finally we would like to minimize the extraneous motion of the joints, and avoid large incremental joint motions that could occur near singularities, that is, $\min_{\Delta \mathbf{q}_m / \Delta t} \|\Delta \mathbf{q}_m / \Delta t\|$.

We can combine the three objective criteria by using a diagonal matrix of weighting factors $W_{m,t}$, $W_{m,s}$ and $W_{m,j}$ associated with each of the objectives. The diagonal elements of $W_{m,t}$ specify the relative importance of each component of the desired Cartesian motion $\Delta \mathbf{x}_m^d$. The ratio of diagonal elements of $W_{m,s}$ to elements of $W_{m,t}$ specify the "stiffness" of the virtual spring connecting the master, and the slave tips. A factor close to zero implies a loose connection or no connection. The ratios between the elements of $W_{m,j}$ themselves can be used to favor motion of some joints over others. We can project the Cartesian tip motion

to the joint motion via the Jacobian J_m , the final objective function is

$$\min_{\Delta \mathbf{q}_m} \left\| \begin{bmatrix} W_{m,t} & \mathbf{0} & \mathbf{0} \\ \mathbf{0} & W_{m,s} & \mathbf{0} \\ \mathbf{0} & \mathbf{0} & W_{m,j} \end{bmatrix} \begin{bmatrix} J_m \\ J_m \\ I \end{bmatrix} \Delta \mathbf{q}_m - \begin{bmatrix} \Delta \mathbf{x}_m^d \\ \Delta \mathbf{x}_{m,s}^e \\ \mathbf{0} \end{bmatrix} \right\| \quad (3)$$

Optimization constraints By defining instantaneous motion relationships between different task frames $\{i\}$ and the incremental joint motions we can implement VF for those task frames. The relationship has the form

$$H_{m,i} J_{m,i}(\mathbf{q}_m) \Delta \mathbf{q}_m \geq \mathbf{h}_{m,i} \quad (4)$$

where $J_{m,i}(\mathbf{q}_m)$ is the Jacobian relating Cartesian task frame vector, $\Delta \mathbf{x}_{m,i}$ to the incremental joint motion. In [17] we had proposed a library of five primitives that could be used to create VF for different tasks by appropriately selecting matrix $H_{m,i}$ and vector $\mathbf{h}_{m,i}$. Our approach allows us to use the basic primitives developed in [17] to a master-slave teleoperator system. Currently we have implemented two sets of constraints for joint limits and joint velocities. The two set of limit constraints can be combined to give the following set of equations

$$H_{m,j} \Delta \mathbf{q}_m \geq \mathbf{h}_{m,j}; \quad \text{where} \quad H_{m,j} = \begin{bmatrix} I \\ -I \\ I \\ -I \end{bmatrix} \quad \text{and} \quad \mathbf{h}_{m,j} = \begin{bmatrix} \mathbf{q}_{m,L} - \mathbf{q}_m \\ \mathbf{q}_m - \mathbf{q}_{m,U} \\ \dot{\mathbf{q}}_{m,U} \cdot \Delta t \\ \dot{\mathbf{q}}_{m,U} \cdot \Delta t \end{bmatrix} \quad (5)$$

where $\mathbf{q}_{m,L}$ and $\mathbf{q}_{m,U}$ are lower and upper bounds of joint ranges and $\dot{\mathbf{q}}_{m,U}$ is the upper bound of the joint velocities. In future we plan to analyze bimanual teleoperation tasks such as knot tying and add additional constraints using this framework.

1.3 Implementation on Slave Manipulator

In this section we discuss objective and constraints for the slave device optimization problem.

Desired Cartesian Motion We define two frames called the neutral frames (denoted by letter N) that are specific tip frames of master and slave, chosen by the user. They are chosen such that the user perceives through the Head Mounted Display (HMD) that the slave gripper is aligned with her hand orientation. We denote the tip frame of the master with respect to a neutral frame as ${}^n F_m = ({}^n R_m, {}^n \mathbf{p}_m)$ and neutral frame of the slave with respect to its base frame as N_s . For the user to always perceive the slave gripper is aligned with her hand, we require that the slave tip motion with respect to its neutral position be same as master tip motion with respect to its neutral. Thus we can write slave tip frame with respect to its base frame as $F_s^d = (R_s^d, \mathbf{p}_s^d) = N_s \cdot {}^n F_m$.

A six vector $\Delta \mathbf{x}_{s,m}^d$ can be computed by taking the difference between the desired frame and the current slave tip frame. The matrix $R_s^e = R_s^d \cdot R_s^{-1}$ can be converted to a three vector by using the Rodriguez formula in (2) or its small angle approximation if applicable. Thus, $\Delta \mathbf{x}_{s,m}^d = [\mathbf{p}_s^d - \mathbf{p}_s; \theta_s \hat{\omega}_s]$. The computation of $\Delta \mathbf{x}_{m,s}^e$ required in (3) can be accomplished by exchanging the roles of master and slave in the above discussion.

Objective function The objective function for the slave has two criteria; one for following the desired motion and the other to restrict extraneous motion of the joints. The final equation is

$$\min_{\Delta \mathbf{q}_s} \left\| \begin{bmatrix} W_{s,t} & \mathbf{0} \\ \mathbf{0} & W_{m,j} \end{bmatrix} \begin{bmatrix} J_s \\ I \end{bmatrix} \Delta \mathbf{q}_s - \begin{bmatrix} \Delta \mathbf{x}_s^d \\ \mathbf{0} \end{bmatrix} \right\| \quad (6)$$

2 Experimental Setup

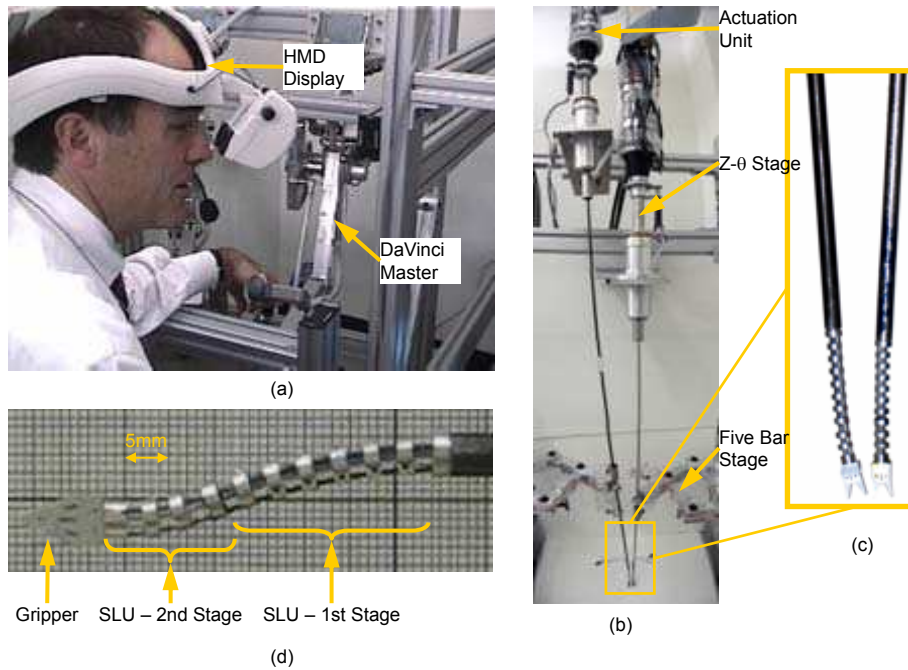


Fig. 2. (a) Master manipulator with HMD display (b) 8-DOF hybrid slave manipulator (c) Closeup of distal end (d) The two SLU's in a bent configuration.

The experimental setup consists of a DaVinci master which is a 7 DOF haptic device, a custom 8 DOF hybrid slave manipulator and a stereo vision system. The master is a commercially available system with its controller replaced by custom hardware and software, thus allowing us greater flexibility in control. The servo loops have a sampling rate of $1kHz$. The devices communicate over TCP network with a sampling rate of $100Hz$, which is the same as the sampling rate for the local high-level control loop. The gains of the PD servo controllers are chosen such that the settling time is less than the sampling rate of master high-level loop. This ensures that the quasi-static approximation required in section 1.2 is met. The vision system consists of a stereo laparoscopic camera mounted at the end of a passive arm. The video streams are displayed on a HMD.

The 8-DOF hybrid slave manipulator is unique and its design was motivated by MIS of the upper airway including the throat and larynx. The slave manipulator consists of two long and slender robotic arms, comprised of a distal end and a proximal end. The distal end consists of two snake-like units (SLU) [1]. Each SLU has four NiTi tubes that use the super-elastic properties of NiTi to allow creation of a slender 2 DOF mechanism. One of these tubes (primary backbone) is located at the center and is connected to all the discs. The other three tubes (secondary backbones) are connected only to the end disc and can slide freely through other discs. The 2 DOF are achieved by pushing or pulling the secondary backbones by three actuators that are located at the proximal end. The second SLU is located at the tip of the first SLU. Inside the backbones of the first SLU, there are three more super elastic NiTi tubes that actuate the second SLU. An additional wire passes through the central backbone to actuate a detachable two-jaw gripper fixed to the end disc of the second SLU. The use of flexible backbone eliminates the need for miniature joints and pulleys. Moreover the redundant push-pull actuation provides actuation redundancy that enhances payload carrying capability. These factors result in a mechanism that is downsize scalable, with our current prototype being $4mm$ in diameter.

Both the robotics arms pass through a laryngoscope that provides access to the patient’s upper airways. In order to avoid obstructing the surgeon’s access, the actuator for the SLU are placed at the end of $1m$ steel tube. The actuator unit is mounted on compact 2 DOF “Z- Θ stage” capable of rotating and translating the actuator units about and along its own axis. The long shaft is supported by a passive universal joint mounted on a 2 DOF five bar mechanism. This provides “X-Y” Cartesian motion at the base of first SLU, and eliminates the lateral deflections of the thin and long shafts.

Though remote actuation of the Distal Dexterity Unit (DDU) has advantages, it introduces modeling problems due to the extension of the actuation lines, friction, and backlash. To achieve faithful control in master-slave mode it is necessary to implement actuation compensation. In a previous work [18] we used a combined model-based with recursive linear estimation approach to obtain the correct actuation compensation. In this actuation compensation approach the required compensation $\epsilon_l = \epsilon(\tau, \mathbf{f}_s, \boldsymbol{\lambda}, \eta)$ is a non-invertible function that depends on the required actuation forces τ of the flexible DDU, together with the static friction \mathbf{f}_s in the actuation lines, and on the vector, $\boldsymbol{\lambda}$, and a scalar η . The vector $\boldsymbol{\lambda}$ accounts for backlash parameters in all actuation lines while the scaling factor η accounts for modeling inaccuracies due to variations in material properties of the backbones and in the bending shape of the snake-like unit. The actuation forces τ are determined through static modeling of the snake-like unit [19] and the friction parameters \mathbf{f}_s are determined empirically. Both $\boldsymbol{\lambda}$ and η are recursively estimated using an external measurement of the orientation of the snake tip such as vision. Using this approach in [18] we successfully demonstrated reducing the tracking errors from more than 45 deg to less than 1 deg . Since ϵ_l is a non-invertible function only an estimate of actual slave frame R_s can be obtained from the estimated lengths of backbones given by $\mathbf{l}^{est} = \mathbf{l}^{enc} + \epsilon_l$ by

applying forward kinematics to l^{est} . Where l^{est} is estimated length and l^{enc} is length measured by encoders in the actuation unit.

3 Results and Discussion

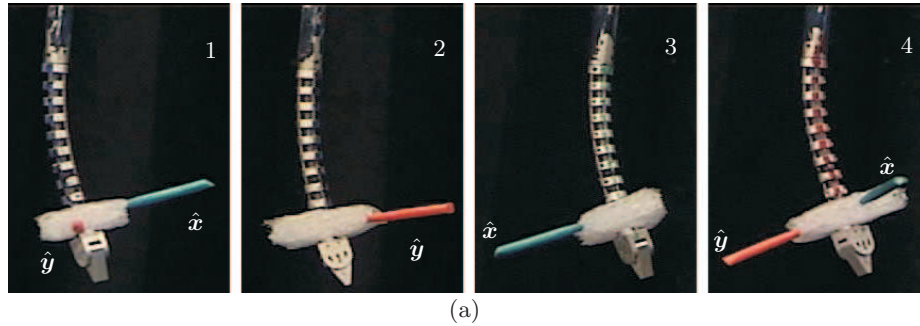


Fig. 3. Series of pictures showing roll motion of gripper. \hat{x} and \hat{y} represent the X and Y axes of gripper frame.

Suturing using a curved needle in confined workspace requires large dexterity at the distal end and sufficient roll about the gripper axis. Figure 3 shows a series of pictures taken during one of these roll motions on one of our earlier prototypes using the control strategy presented in [15]. This has a potential benefit in laryngeal surgery as multiple instruments need to be used through a narrow opening of the laryngoscope. Thus, little or no motion of joints at the proximal end minimizes tool collision and gives the surgeon sufficient access to the surgical site. We are currently evaluating this setup with a simple suturing phantom for *ex vivo* suturing.

4 Conclusions and Future Work

We have presented the high-level control of a telesurgical system designed considering the special requirements of MIS of throat. The high level control is based on linearized constraints, multi-objective least square optimization problem that is easily extendable to include additional constraints such as collision avoidance, anatomic-based constraints [14] and joint limits.

The dexterity of the SLU was effectively used to provide roll movement of the gripper, without any motions of the proximal joints. This is a crucial requirement for suturing in confined spaces, such as the throat.

The current results serve as a validation of our control to be used in the novel telerobotic system for MIS of the throat. The current work also provides a basis for implementing virtual fixtures in impedance-type robots for complex tasks such as suturing.

Acknowledgements

This work was partially funded by the National Science Foundation (NSF) under Engineering Research Center grant #EEC9731478, NSF grant #IIS9801684 and National Institutes of Health (NIH) grant #R21 B004457-01 and by Columbia University and Johns Hopkins University internal funds. The authors are also thankful for the guidance and support of Dr. Paul Flint.

References

1. Simaan, N., et al.: High dexterity snake-like robotic slaves for minimally invasive telesurgery of the upper airway. In: MICCAI. (2004) 17–24
2. Peirs, J., et al.: Design of an advanced tool guiding system for robotic surgery. In: ICRA. (2003) 2651–2656
3. Takahashi, H., et al.: Development of high dexterity minimally invasive surgical system with augmented force feedback capability. In: BioRob. (2006)
4. Ikuta, K., et al.: Development of remote microsurgery robot and new surgical procedure for deep and narrow space. In: ICRA. (2003) 1103 – 1108
5. Charles, S., et al.: Dexterity-enhanced telerobotic microsurgery. In: ICAR. (1997) 5–10
6. Csencsits, M., et al.: User interfaces for continuum robot arms. In: IROS. (2005) 3123 – 3130
7. Davies, B.L., et al.: Active compliance in robotic surgery the use of force control as a dynamic constraint. Proc Inst Mech Eng [H]. **211**(4) (1997) 285–292
8. Marayong, P., et al.: Spatial motion constraints: Theory and demonstrations for robot guidance using virtual fixtures. In: ICRA. (2003) 1954–1959
9. Rosenberg, L.B.: Virtual fixtures: Perceptual tools for telerobotic manipulation. In: IEEE Virtual Reality Annual International Symposium. (1993) 76–82
10. Park, S., et al.: Virtual fixtures for robotic cardiac surgery. In: MICCAI. (2001) 1419 – 1420
11. Turro, N., Khatib, O.: Haptically augmented teleoperation. In: Intl. Symposium on Experimental Robotics. (2000) 1–10
12. Abbott, J.J., Okamura, A.M.: Analysis of virtual fixture contact stability for telemanipulation. In: IROS. (2003) 2699 – 2706
13. Funda, J., et al.: Constrained cartesian motion control for teleoperated surgical robots. IEEE Trans. Robot. Automat. **12**(3) (1996) 453–465
14. Li, M., Taylor, R.H.: Spatial motion constraints in medical robot using virtual fixtures generated by anatomy. In: ICRA. (2004) 1270–1275
15. Kapoor, A., et al.: Suturing in confined spaces: Constrained motion control of a hybrid 8-dof robot. In: ICAR. (2005) 452 – 459
16. Abbott, J.J., et al.: Steady-hand teleoperation with virtual fixtures. In: 12th IEEE Workshop on Robot and Human Interactive Communication. (2003) 145–151
17. Li, M., et al.: A constrained optimization approach to virtual fixtures. In: IROS, Edmonton, Canada (2005) 1408 – 1413
18. Xu, K., Simaan, N.: Actuation compensation for flexible surgical snake-like robots with redundant remote actuation. In: ICRA. (2006) 4148–4154
19. Simaan, N.: Snake-like units using flexible backbones and actuation redundancy for enhanced miniaturization. In: ICRA. (2005) 3020–3028